Reactions of $H_3Al{\cdot}NMe_3$ with $E(SiMe_3)_3$ (E = P, As). Structural Characterization of the Trimer $[H_2AlP(SiMe_3)_2]_3$ and Base-Stabilized Adduct $[H_2AlAs(SiMe_3)_2]{\cdot}NMe_3$ and Their Thermal Decomposition toward Nanocrystalline AlP and AlAs, Respectively

Jerzy F. Janik† and Richard L. Wells*

Department of Chemistry, Paul M. Gross Chemical Laboratory, Duke University, Durham, North Carolina 27708-0346

Peter S. White

Department of Chemistry, University of North Carolina at Chapel Hill, Chapel Hill, North Carolina 27514

Received February 27, 1998

Dehydrosilylation reactions in diethyl ether between $H_3Al{\cdot}NMe_3$ and $E(SiMe_3)_3$ afforded for E = P a high yield of the trimer $[H_2AlP(SiMe_3)_2]_3$ (**1**), while for E = As a monomeric base-stabilized adduct $[H_2AlAs(SiMe_3)_2]{\cdot}NMe_3$ (**2**) as well as its degradation solid product were obtained. No reaction occurred for E = N. The single-crystal X-ray structure determination for **1** yielded a planar six-membered ring of alternating four-coordinated Al and P centers. The structural solution for **2** revealed the monomeric unit $[H_2AlAs(SiMe_3)_2]$ stabilized by coordination of NMe_3 at the Al site. Pyrolysis of **1** at 450 °C promoted further dehydrosilylation and yielded a product which by XRD spectroscopy showed the onset of AlP crystallinity while at 950 °C afforded nanocrystalline AlP with 5 nm average particle size. Pyrolysis of **2** at 450 °C resulted in the formation of nanocrystalline AlAs with 2 nm average particle size. Under applied pyrolysis conditions for **1** and **2**, the target elimination−condensation pathway via dehydrosilylation was accompanied by other decomposition side reactions and retention of some contaminant residues.

Introduction

Dehydrosilylation elimination−condensation reactions are characterized by a commonly facile evolution of volatile $HSiMe_3$ with concurrent formation of the M(13)−E(15) bond according to the scheme $\{R^1M(13)\} + \{E(15)R^2\} = \{M(13)-E(15)\} + HSiMe_3$ (R^1, R^2 = H, $SiMe_3$ or R^1, R^2 = $SiMe_3$, H); however, only a few reports seem to have been published in this area.[1] Regarding this chemistry, we have reported on a number of occasions our studies on dehydrosilylation as a means for making 13−15 bonds and formation of potential precursors to 13−15 ceramic and semiconductor materials.[2] Thus, the reactions between $LiGaH_4$ and $E(SiMe_3)_3$ (E = P, As) afford new lithium pnictidogallates, $(Et_2O)_2Li[\mu\text{-}E(SiMe_3)_2]_2GaH_2$, featuring a planar four-membered ring in which the Li and Ga atoms are bridged by two E atoms.[2a] Similarly, the reactions of $LiAlH_4$ and $E(SiMe_3)_3$ (E = P, As) yield lithium pnictidoaluminates, $(Et_2O)_2Li[\mu\text{-}E(SiMe_3)_2]_2AlH_2$, structurally isomorphous with their gallium counterparts.[2b] The new lithium pnictidometalates may be useful starting materials for mixed-metal derivatives containing two different group 13 elements which, upon further elimination−condensation, could lead to ternary (or higher) 13−15 materials.

An extension of this chemistry to the system $H_3Ga{\cdot}NMe_3$/$E(SiMe_3)_3$ (E = P, As) has also been fruitful and resulted in the trimers $[H_2GaE(SiMe_3)_2]_3$—the rare examples of a phosphinogallane and arsinogallane containing GaH_2, the parent gallane functionality.[2c] Prior to that, the related phosphinoborane $[H_2BP(SiMe_3)_2]_3$ was isolated from the system $H_3B{\cdot}THF/P(SiMe_3)_3$[1a] and phosphinogallane $(H_2GaPCy_2)_3$ was made via salt elimination from the combination of $H_2(Cl)Ga{\cdot}PCy_3$ and $LiPCy_2{\cdot}n$THF (Cy = cyclohexyl).[3a] Interestingly, the structures of all three trimers containing four-coordinated group 13 and $SiMe_3$-bound group 15 atoms show significant ring flattening or planarity. They also display curious incidents of the thermal parameters for the group 13 atom being about twice the magnitude of the group 15 atom, yet both atoms occupy structurally similar positions in the ring. This property, which could be linked to deviations from ring planarity, appears to be a specific feature in this family of compounds. That the reasons behind it are not quite obvious is illustrated by the structural solution for the sterically similar trimer $[t\text{-}Bu_2GaPH_2]_3$ which provides a planar ring core while thermal parameters for Ga and P appear to be

* To whom correspondence should be addressed.

† On leave from the University of Mining and Metallurgy, Krakow, Poland.

(1) For example, see: (a) Wood, G. L.; Dou, D.; Narula, C. K.; Duesler, E. N.; Paine, R. T.; Nöth, H. *Chem. Ber.* **1990**, *123*, 1455 and references therein. (b) Janik, J. F.; Duesler, E. N.; Paine, R. T. *Inorg. Chem.* **1987**, *26*, 4341. (c) Janik, J. F.; Duesler, E. N.; McNamara, W. F.; Westerhausen, M.; Paine, R. T. *Organometallics* **1989**, *8*, 506.

(2) (a) Janik, J. F.; Wells, R. L.; Young, V. G., Jr., Halfen, J. A. *Organometallics* **1997**, *16*, 3022. (b) Janik, J. F.; Wells, R. L.; White, P. S. *Organometallics* **1998**, in press. (c) Janik, J. F.; Wells, R. L.; Young, V. G., Jr.; Rheingold, A. L.; Guzei, I. A. *J. Am. Chem. Soc.* **1998**, *120*, 532.

(3) (a) Elms, F. M.; Koutsantonis, G. A.; Raston, C. L. *J. Chem. Soc., Chem. Commun.* **1995**, 1669. (b) Cowley, A. H.; Harris, P. R.; Jones, R. A.; Nunn, C. M. *Organometallics* **1991**, *10*, 652.

S0020-1669(98)00218-3 CCC: $15.00
Published on Web 07/13/1998

comparable.[3b] More structural data are clearly needed to better understand these phenomena.

The cases discussed above reveal that oligomerization of the likely transient monomeric unit formed upon dehydrosilylation, $[H_2ME(SiMe_3)_2]$, is favored over plausible stabilization of the monomer with the available NMe_3, a potent Lewis base. However, there are known cases which yield base-stabilized adducts, instead. For example, dihydrogen elimination from the combinations of $H_3Al{\cdot}NMe_3$ or $H_2ClAl{\cdot}NMe_3$ and $HN(SiMe_3)_2$ is reported to yield $[H_2AlN(SiMe_3)_2]{\cdot}NMe_3$[4] or $[H(Cl)AlN(SiMe_3)_2]{\cdot}NMe_3$,[4c] respectively. The preference of the base-stabilized adducts over oligomerization products in these cases could perhaps be linked to a mere latent basicity of the nitrogen atom in $N(SiMe_3)_2$, the property that could further be enhanced by steric congestion imposed by this ligand; to the best of our knowledge, there have not been reported ring structures featuring bridging $N(SiMe_3)_2$ groups. Other examples include salt-elimination reactions in the system $LiE(Mes)_2/H_2ClAl{\cdot}NMe_3$ (E = P, As), which also result in the base-stabilized adducts $[H_2AlEMes_2]{\cdot}NMe_3$.[5] All these cases do not provide, however, sufficient comparative data to understand the outcome of the reactions in systems containing a strong Lewis base as is the case of the convenient forms of alane and gallane, $H_3M{\cdot}NMe_3$ (M = Al, Ga).

Herein we describe reactivity in the systems $H_3Al{\cdot}NMe_3/E(SiMe_3)_3$, E = N, P, and As, and the formation and structural characterization of the trimer $[H_2AlP(SiMe_3)_2]_3$ (**1**) and monomeric base-stabilized adduct $[H_2AlAs(SiMe_3)_2]{\cdot}NMe_3$ (**2**); the latter compound, if not isolated and stored at −30 °C, spontaneously decomposes to a white insoluble solid. We conclude this report with preliminary results of the pyrolyses of **1** and **2** that yield nanocrystalline AlP and AlAs, respectively.

Experimental Section

General Techniques. All experiments were carried out using standard vacuum/Schlenk techniques.[6] Solvents were dried and distilled from Na benzophenone ketyl or Na/K alloy prior to use. $N(SiMe_3)_3$ was purchased from Aldrich and used as received. $H_3Al{\cdot}NMe_3$,[7] $P(SiMe_3)_3$,[8] and $As(SiMe_3)_3$[9] were prepared by the literature methods. ^1H, $^{13}C\{^1H\}$, and ^{31}P NMR spectra were acquired on a Varian Unity 400 spectrometer at 25 °C from toluene-d_8 or benzene-d_6 solutions and referenced vs $SiMe_4$ by generally accepted methods. Mass spectra were collected on a JEOL JMS-SX 102A spectrometer operating in the EI mode at 20 eV; the CI mode (isobutane) yielded comparable results. IR spectra of solids and gaseous pyrolysis products were acquired using KBr pellets and a gas cell, respectively, on a BOMEM Michelson MB-100 FT-IR spectrometer. A calibrated manifold was used for volume estimations of reaction gases. Elemental analyses were provided by E+R Microanalytical Laboratory, Corona, NY. Melting behavior (uncorrected) was determined with a Thomas-Hoover Uni-melt apparatus for samples flame-sealed in glass capillaries. TGA/DTA analyses were performed under a UHP nitrogen flow and 5 °C/min heating rate on a TA Instruments SDT 2960 simultaneous TGA/DTA apparatus. Single-crystal X-ray diffraction studies for **1** (223 K) and **2** (173 K) were performed at the University of North Carolina at Chapel Hill, Chapel Hill, NC, on a Siemens SMART Platform CCD system using Mo Kα radiation (λ = 0.710 73 Å). All calculations were carried out with the help of NRCVAX programs;[10] the structures were solved by direct methods. XRD data for powders were collected using mineral oil coated samples on a Phillips XRD 3000 diffractometer utilizing Cu Kα radiation; the average particle sizes of the AlP and AlAs products were calculated using the Scherrer equation applied to the (111) diffraction lines of the cubic AlP (JCPDS file 12-470) and cubic AlAs (JCPDS file 17-915).

Reaction System $H_3Al{\cdot}NMe_3/P(SiMe_3)_3$ in Et_2O. (1) Synthesis and Characterization of $[H_2AlP(SiMe_3)_2]_3$ (1). A sample of freshly prepared $H_3Al{\cdot}NMe_3$, 0.54 g or 6.0 mmol, was dissolved in 20 mL of Et_2O, and a solution of $P(SiMe_3)_3$ in 20 mL of Et_2O, 1.50 g or 6.0 mmol, was added to it at room temperature. Several minutes after addition, the mixture turned slightly milky. It was stirred at ambient conditions overnight, some white insoluble solid filtered out, and the filtrate concentrated by evacuation to a few milliliters. After 2−3 days at −30 °C, abundant colorless crystals of **1** appeared, 0.85 g or 69% yield based on eq 1 (vide infra); even more crystals could be recovered upon further workup of the solution. Melting behavior: 70−150 °C, visible decomposition with massive gas evolution; above 200 °C, change of color to yellow and golden-red; no melting to 300 °C. Anal. Found (calcd) for $C_{18}H_{60}Al_3P_3Si_6$: C, 34.65 (34.92); H, 9.60 (9.77). ^1H NMR (toluene-d_8): δ 0.481, 0.485, 0.489, 0.493 (equally spaced four-line multiplet with relative intensities 80:100:100:80 and separation of 1.7 Hz, 54H; $SiMe_3$), 4.4 (6H, br; AlH_2). $^{13}C\{^1H\}$ NMR (tolune-d_8) (intensity): four-line multiplet at δ 2.44 (sh, 70), 2.47 (100), 2.49 (100), 2.52 (sh, 60); $SiMe_3$. $^{31}P\{^1H\}$ NMR (toluene-d_8): δ −273.5. MS [*m*/*e* (intensity) (ion)]: peak clusters around 617 (5) ($[H_2AlP(SiMe_3)_2]_3$ − H or M − H), 588 (2) (M − 2Me), 543 (13) (M − $SiMe_3$ − 2H), 514 (7) (M − $SiMe_3$ − 2Me − H), 441 (55) (M − $P(SiMe_3)_2$), 412 (100) ($[H_2AlP(SiMe_3)_2]_2$ or M*), 397 (9) (M* − Me), 367 (57) (M* − 3Me), 351 (30) (M* − 4Me − H), 338 (100) (M* − $SiMe_3$ − H), 323 (36) (M* − $SiMe_3$ − Me − H), 309 (16) (M* − $SiMe_3$ − 2Me), 293 (21) (M* − $SiMe_3$ − 3Me − H), 279 (51) (M* − $SiMe_3$ − 4Me), 264 (78) (M* − $2SiMe_3$ − 2H), 249 (18) (M* − $2SiMe_3$ − Me − 2H), 234 (18) (M* − $2SiMe_3$ − 2Me − 2H), 205 (26) ($H_2AlP(SiMe_3)_2$ − H or M** − H), 191 (M** − Me), 178 (38) ($HP(SiMe_3)_2$), 174 (23) (M** − 2Me − 2H), 163 (21) ($HP(SiMe_3)_2$ − Me), 160 (16) (M** − 3Me − H), 73 (61) ($SiMe_3$), 59 (4) ($HSiMe_2$). IR: ν(Al−H) 1796 cm^{-1}. Note, the NMR spectra for raw decanted crystals of **1** show also resonances for some residual $P(SiMe_3)_3$ as well as a set of apparently correlated signals in the ^1H NMR spectrum at δ 0.504 (that could be a part of a doublet partially buried under the major four-line multiplet) and 1.89 (s; NMe_3) which seem to correspond to the $^{13}C\{^1H\}$ NMR resonances at δ 4.96 (d, $^2J_{P-C}$ = 10.7 Hz; $SiMe_3$) and 47.4 (s; NMe_3) in a minor byproduct.

(2) Thermal Decomposition. Significant TGA weight changes commenced at 60 °C and exhibited one major weight loss to 250 °C, 55%, followed by a smaller loss to 450 °C, 3.5%; total weight loss of 58.5%. Calculated weight loss for $[H_2AlP(SiMe_3)_2]_3$ = 3AlP + $6HSiMe_3$, 71.9%. A sample of **1**, 0.40 g or 0.65 mmol, was pyrolyzed in a sublimer for 2 h at 450 °C under vacuum and with the collection of volatiles. Small quantities of a colorless, oily liquid, likely $P(SiMe_3)_3$, distilled out onto colder parts of the setup together with brown solid deposits which were additionally observed after completion of pyrolysis. Also, the inner surface of the sublimer was deposited with a shiny, coppertone-like solid film which could not easily be removed afterward. The major product was a brown solid, 0.10 g or weight loss of 75%: noncondensables (CH_4 and H_2), 0.9 mmol; condensables ($HSiMe_3$), 2.5 mmol; weight of volatiles, approximately 0.2 g. An XRD pattern for the brown product showed two extremely broad features at 2θ 30° and 50° consistent with the onset of AlP crystallinity; average particle size, < 1 nm. A similar pyrolysis experiment was carried out at 950 °C without the collection of volatiles. A dark gray/black solid product was obtained whose XRD spectrum matched JCPDS file 12-470 for cubic AlP; average particle size, 5 nm. EA: Al, 28.62; P, 33.53; Si,

(4) (a) Janik, J. F.; Paine, R. T. Presented at the XVth International Conference on Organometallic Chemistry, Warsaw, Poland, Aug 1992, P113. (b) Janik, J. F.; Duesler, E. N.; Paine, R. T. *J. Organomet. Chem.* **1997**, *539*, 19. (c) Gardiner, M.; Koutsantonis, G. A.; Lawrence, S. M.; Lee, F.-C.; Raston, C. L. *Chem. Ber.* **1996**, *129*, 545.
(5) Atwood, D. A.; Contreras, L.; Cowley, A. H.; Jones, R. A.; Mardones, M. A. *Organometallics* **1993**, *12*, 17.
(6) Shriver, D. F.; Drezdzon, M. A. *The Manipulation of Air Sensitive Compounds*; Wiley-Interscience: New York, 1986.
(7) Kovar, R. A.; Callaway, J. O. *Inorg. Synth.* **1977**, *17*, 36.
(8) Becker, G.; Hölderich, W. *Chem. Ber.* **1975**, *108*, 2484.
(9) (a) Becker, G.; Gutenkunst, G.; Wessely, H. J. *Z. Anorg. Allg. Chem.* **1980**, *462*, 113. (b) Wells, R. L.; Self, M. S.; Johansen, J. D.; Laske, J. A.; Aubuchon, S. R.; Jones, L. J. *Inorg. Synth.* **1997**, *31*, 150.
(10) Gabe, E. J.; Le Page, Y.; Charland, J.-P.; Lee, F. L.; White, P. S. *J. Appl. Crystallogr.* **1989**, *22*, 384.

11.31; C, 4.69; H, 0.62; P/Al = 1.02; C/Si = 0.97. Also, the whole length of the pyrolysis tube was vapor-deposited inside with a thin and shiny, goldenlike solid film.

Reaction System $H_3Al{\cdot}NMe_3/As(SiMe_3)_3$ in Et_2O. (1) Synthesis and Characterization of $[H_2AlAs(SiMe_3)_2]{\cdot}NMe_3$ (2). Typically, a sample of freshly prepared $H_3Al{\cdot}NMe_3$, 0.45 g or 5.0 mmol, was dissolved in 20 mL of Et_2O, and a solution of $As(SiMe_3)_3$ in 20 mL of Et_2O, 1.47 g or 5.0 mmol, was added to it at room temperature. The mixture turned milky several minutes after addition. It was stirred overnight, and a relatively small quantity of the insoluble solid was filtered out; the solution was concentrated by evacuation to a few milliliters and stored at −30 °C. After 4 weeks under these conditions only some insoluble white solid precipitated. Sizable quantities of crystalline **2** were obtained by either of the two following methods. First, **2** crystallized from the original Et_2O solution that was subsequently evacuated almost entirely in the course of several hours at −30 °C. Alternatively, the ether was removed from a portion of the original mixture, the solids redissolved in toluene, and the concentrated solution stored in an opened vial at −30 °C (dry-lab freezer); such a slow evaporation of the solvent in the course of several days afforded abundant colorless crystals of **2**. X-ray-quality crystals were obtained at −30 °C. They were coated with a protective oil prior to structure determination. For other characterization purposes and to remove excess of oily $As(SiMe_3)_3$, the crystalline solid was briefly washed with cold hexane and evacuated for a few minutes. Melting point: 68−70 °C, clear liquid. Anal. Found (calcd) for $C_9H_{29}NAlAsSi_2$: C, 34.62 (34.94); H, 9.28 (9.45); N, 4.29 (4.53). ^{1}H NMR (toluene-d_8/benzene-d_6): δ 0.56/0.61 (18H; $SiMe_3$), 2.01/1.85 (9H, NMe_3), 4.0/4.0 (2H, very broad; AlH_2). $^{13}C\{^1H\}$ NMR (toluene-d_8) (intensity; assignment): δ 5.2 (70; $SiMe_3$); 47.3 (100; NMe_3). MS [*m*/*e* (intensity) (ion)]: peak clusters around 309 (8) ($[H_2AlAs(SiMe_3)_2]{\cdot}NMe_3$ or M), 294 (100) (M − Me or $As(SiMe_3)_3$), 279 (16) (M − 2Me or $As(SiMe_3)_3$) − Me), 250 (2) (M − NMe_3), 222 (40) ($HAs(SiMe_3)_2$), 206 (43) (M − NMe_3 − 3Me + H), 191 (7) (M − NMe_3 − 4Me + H), 177 (3) (M − NMe_3 − $SiMe_3$), 147 (6) (M − NMe_3 − $SiMe_3$ − 2Me), 134 (6) ($SiAsAlH_4$), 73 (63) ($SiMe_3$), 59 (8) ($HSiMe_2$). IR: ν(Al−H) 1784 cm^{-1}. Note, the insoluble decomposition product of **2** that was obtained from the reaction mixture upon long storage showed by IR spectrometry a broad stretch ν(Al−H) at 1795 cm^{-1}.

(2) Thermal Decomposition. A sample of **2**, 0.71 g or 2.3 mmol, was pyrolyzed in a sublimer for 2 h at 450 °C under vacuum and with the collection of volatiles. Small quantities of a colorless, oily liquid, likely $As(SiMe_3)_3$, distilled out. Additionally, after completion of pyrolysis, some colored solids were found on the colder parts of the setup. The solid pyrolysis product was a dark gray/black solid, 0.25 g or weight loss 65%: noncondensables (CH_4 and H_2), 1.5 mmol; condensables ($HSiMe_3$ and NMe_3), 5.1 mmol; weight of volatiles, approximately 0.3 to 0.4 g. A XRD pattern for the black product showed very broad peaks consistent with the onset of AlAs crystallinity; average particle size, approximately 2 nm. EA for the black product: Al, 37.96; As, 59.18; C, 0.38; H, 0.67; Si (by difference), 1.81; Al/As = 1.78.

Structural Determinations for 1 and 2. Specimens of **1** and **2** were stored at −30 °C prior to determinations. The intensity data were collected on a Siemens SMART diffractometer using the ω scan mode. For **1**, systematic absences and diffraction symmetry indicated the trigonal space group $P\bar{3}$; cell dimensions were obtained from 5558 reflections with 2θ 3.00−50.00°. For **2**, the data determined the monoclinic space group $P2_1$; cell dimensions were obtained from 6832 reflections with 2θ 3.00−50.00°. The structures were solved by direct methods. All non-hydrogen atoms were refined with anisotropic displacement parameters. All hydrogen atoms, including Al hydrogens, were placed in ideal positions and refined as riding atoms with relative isotropic displacement parameters. The Al−H bond length was assumed at 1.50 Å. Details of the data collection for **1** and **2** are summarized in Table 1, and Table 2 shows selected bond distances and angles.

Table 1. Crystallographic Data and Measurements for 1 and 2.

	1	**2**
molecular formula	$C_{18}H_{60}Al_3P_3Si_6$	$C_9H_{29}AlAsSi_2N$
formula weight	619.05	309.41
crystal system	trigonal	monoclinic
space group	$P3$	$P2_1$
a, Å	11.8152(7)	9.1285(5)
b, Å		11.1657(6)
c, Å	16.7019(10)	9.1283(6)
β, deg		104.274(1)
V, Å^3	2019.20(17)	901.69(9)
Z	2	2
μ, mm^{-1}	0.40	2.04
temp, K	223(2)	173(2)
D_{calcd}, g/cm^3	1.018	1.140
cryst dimens, mm	0.25 × 0.25 × 0.15	0.20 × 0.20 × 0.35
θ range for data collcn (deg)	1.50−25.00	1.50−25.00
no. of rflns collcd	17 793	7955
no. of unique rflns	2417	3173
no. of rflns ($I > 2.5\sigma(I)$)	1916	2823
R ($I > 2.5\sigma(I)$);[a] R_w[b]	0.066; 0.079	0.048; 0.057
R (all data);[a] R_w[b]	0.101; 0.105	0.054; 0.060
goodness-of-fit[c]	4.46	2.44
final max/min $\Delta\rho$, e/Å^{-3}	0.390/−0.400	1.45/−0.820

[a] $R = \sum||F_o| - |F_c||/\sum|F_o|$. [b] $R_w = [\sum w(|F_o| - |F_c|)^2/\sum w|F_o|^2]^{1/2}$. [c] GooF = $[\sum[w(|F_o| - |F_c|)^2]/(n - p)]^{1/2}$.

Results and Discussion

The combination of $H_3Al{\cdot}NMe_3$ and $P(SiMe_3)_3$ in diethyl ether at ambient conditions resulted in a high yield of the dehydrosilylation product, trimer $[H_2AlP(SiMe_3)_2]_3$ (**1**), as described in eq 1.

$$H_3Al{\cdot}NMe_3 + P(SiMe_3)_3 \xrightarrow{Et_2O} {}^1/_3[H_2AlP(SiMe_3)_2]_3 + HSiMe_3 + NMe_3 \quad (1)$$

Such an outcome was expected on the basis of the trimeric nature of products from other related systems such as $H_3Ga/E(SiMe_3)_3$ (E = P, As)[2c] and $H_3B{\cdot}THF/P(SiMe_3)_3$.[1a] On the other hand, a reaction between $H_3Al{\cdot}NMe_3$ and $As(SiMe_3)_3$ under comparable conditions yielded a different dehydrosilylation product, base-stabilized monomer $[H_2AlAs(SiMe_3)_2]{\cdot}NMe_3$ (**2**), according to the following equation:

$$H_3Al{\cdot}NMe_3 + As(SiMe_3)_3 \xrightarrow{Et_2O} [H_2AlAs(SiMe_3)_2]{\cdot}NMe_3 + HSiMe_3 \quad (2)$$

Interestingly, two related P and As derivatives $[H_2AlEMes_2]{\cdot}NMe_3$ (E = P, As)[5] were both base-stabilized adducts. Although it is tempting in these cases to speculate on the significance of such intrinsic bonding factors as bond strength and/or steric influence, it may simply be that variations in reaction conditions are responsible for the nature of the isolated product, i.e., oligomer or base-stabilized adduct. We note that for E = P there was a NMR evidence for a minor byproduct containing a coordinated NMe_3 molecule and this could be a transient or coexisting with **1** based-stabilized $[H_2AlP(SiMe_3)_2]{\cdot}NMe_3$. In this regard, the related $[H_2AlPMes_2]{\cdot}NMe_3$ was reported to lose NMe_3 when heated under vacuum and convert to the proposed species of empirical formula $[H_2AlPMes_2]_n$. We, too, noticed a similar effect for $[H_2AlAs(SiMe_3)_2]{\cdot}NMe_3$ upon its prolonged evacuation at ambient conditions; however, an accompanying decomposition associated with the formation of $As(SiMe_3)_3$ prevented us from isolation of well-defined byproduct(s). In yet another relevant report, heating $[H_2AlN(SiMe_3)_2]{\cdot}NMe_3$[4a,b] appeared to result in disproportionation chemistry rather than simple removal of the coordinated amine. Finally, no reaction was detected in this study between $H_3Al{\cdot}NMe_3$ and $N(SiMe_3)_3$

Table 2. Selected Bond Distances (Å) and Angles (deg) for **1** and **2** with Estimated Standard Deviations in Parentheses

1		**2**	
	Bond Lengths		
P(1)−Al(1)	2.3916(16)	As(1)−Al(1)	2.4383(21)
P(1a)−Al(1)	2.4041(14)	Al(1)−N(1)	1.998(7)
P−Si(av)	2.263	As−Si(av)	2.344
Si−C(av)	1.840	Si−C(av)	1.865
Si−C(min/max)	1.832(8)/1.849(8)	Si−C(min/max)	1.850(9)/1.883(7)
	Bond Angles		
P(1)−Al(1)−P(1a)	113.58(8)	As(1)−Al(1)−N(1)	105.90(19)
Al(1)−P(1)−Al(1b)	126.42(7)	Si(1)−As(1)−Si(2)	104.82(7)
Si(1)−P(1)−Si(2)	107.83(8)	Al−N−C(av)	109.8
Al−P−Si(av)	105.4	Al−As−Si(av)	96.7
P−Al−H(av)	108.4	As−Si−C(av)	110.4
	Torsion Angles		
Al(1)−P(1)−Si(1)−C(13)	173.5(6)	Si(1)−As(1)−Al(1)−N(1)	−127.2(3)
Al(1)−P(1)−Si(2)−C(23)	−173.4(6)	Si(2)−As(2)−Al(1)−N(1)	126.9(3)
Al(1)−P(1)−Si(2)−C(22)	65.9(4)	As(1)−Al(1)−N(1)−C(2)	179.8(8)

even after reflux in Et_2O in accord with a rather notorious lack of reactivity of this amine toward $HSiMe_3$ elimination, as reported earlier from this laboratory.[2] It is interesting to note, however, that $N(SiMe_3)_3$ underwent Me_3SiCl elimination reactions with haloboranes.[11]

Trimer **1** appeared to be quite stable at room temperature, at least after isolation and in toluene solutions. Under these conditions, it was decomposing slowly with the formation of free $P(SiMe_3)_3$ and $HSiMe_3$. For example, by NMR spectroscopy, after 3 weeks approximately 25% of it had decayed. Under comparable conditions, the NMR toluene-d_8 solution of **2** was barely decomposed after 2 weeks with only traces of $HSiMe_3$ and possible $As(SiMe_3)_3$ formed. This kind of stability of isolated **2** was somewhat surprising since if **2** was left in the mother liquor it would have turned rather fast to an insoluble solid. Generally, pnictinoalane derivatives **1** and **2** showed higher stabilities than the related pnictinogallane trimers $[H_2GaE(SiMe_3)_2]_3$ (E = P, As);[2c] in the latter cases, the evolution of dihydrogen was additionally observed due to the higher thermal frailty of the Ga−H bond.

The elemental analysis for compound **1** was consistent with the stoichiometry of $\{H_2AlP(SiMe_3)_2\}$. Such a makeup was supported also by the ^1H NMR resonance at δ 4.4, in the range expected for protons in the AlH_2 groups. The presence of such groups in **1** was further corroborated by its IR spectrum displaying an Al−H stretching band at 1796 cm^{-1}. The remaining NMR data for the compound were of somewhat limited value in elucidating structural features. Both ^1H and $^{13}C\{^1H\}$ NMR spectra showed regularly spaced four-line multiplets for protons and carbons in the $SiMe_3$ groups, respectively, suggesting a complex structure in solution. This information however excluded a planar dimer where virtual triplets would have been expected. Interestingly, the ^1H NMR spectrum for the closely related gallium derivative $[H_2GaP(SiMe_3)_2]_3$ displayed a broadened doublet for the $SiMe_3$ protons.[2c] Strong support for the trimeric species in the gaseous state was provided by mass spectrometry. The spectrum contained the molecular ion for the species $\{[H_2AlP(SiMe_3)_2]_3 - H\}$ as the highest *m*/*e* cluster and other logical fragments.

The elemental analysis for compound **2** supported its formulation as the monomeric base-stabilized adduct $[H_2AlAs(SiMe_3)_2]\cdot NMe_3$. The presence of the coordinated NMe_3 in **2** was substantiated by the ^1H and $^{13}C\{^1H\}$ NMR spectra in toluene-d_8 which showed the resonances at δ 2.01 and 47.3, respectively, for the amine. The ^1H NMR spectrum contained also a singlet in the $SiMe_3$ region and an extremely broad signal at approximately δ 4.0. The latter resonance was consistent with the presence of the AlH_2 moiety as was the infrared Al−H stretching band observed at 1784 cm^{-1}. Further corroboration of the structure was provided by mass spectrum for **2** which showed the expected molecular ion at *m*/*e* 309.

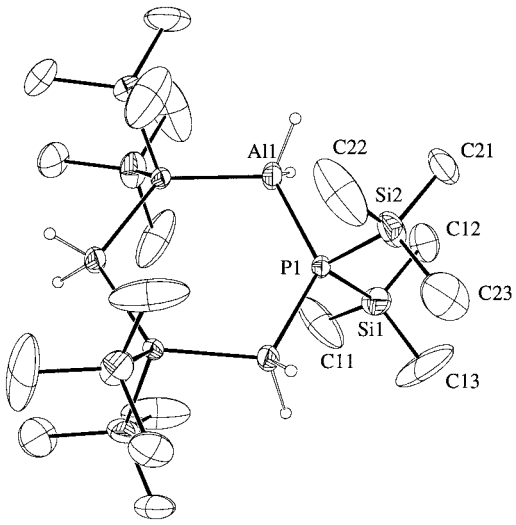

Figure 1. Thermal ellipsoid diagram (35% probability ellipsoids) showing the molecular structure of **1**. All carbon−hydrogen atoms are omitted for clarity.

The solid-state structures of compounds **1** and **2** were authenticated by single-crystal X-ray structure determinations. Figure 1 shows the thermal ellipsoid diagram for compound **1**. The structure is solved as a planar six-membered ring of alternating four-coordinated Al and P atoms. Its major features, although interesting, are not novel in that they match those found in three other related trimers, $[H_2GaE(SiMe_3)_2]_3$ (E = P, As)[2c] and $[H_2BP(SiMe_3)_2]_3$.[1a] For example, the thermal parameters for the Al atom in **1** are about twice the magnitude of the P atom, in accord with the trend in this family of compounds. As mentioned earlier, this may be indicative of the molecular symmetry of **1** being lower than the crystallographic site symmetry and the ring probably not planar. Similarly, the ring Al−P−Al angle, 126.42(7)°, is larger the corresponding P−Al−P angle, 113.58(8)°, which is also true for the respective angles at group 13 and 15 atoms in the related compounds. The Al−P

(11) For example, see: (a) Janik, J. F.; Narula, C. K.; Gulliver, E. G.; Duesler, E. N.; Paine, R. T. *Inorg. Chem.* **1988**, *27*, 1222. (b) Barlos, K.; Christl, H.; Nöth, H. *Liebigs Ann. Chem.* **1976**, 2272. (c) Srivastava, G. *J. Organomet. Chem.* **1974**, *69*, 179.

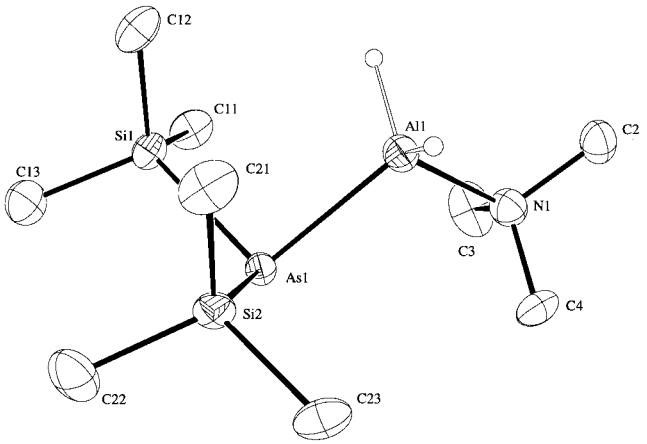

Figure 2. Thermal ellipsoid diagram (35% probability ellipsoids) showing the molecular structure of **2**. All carbon−hydrogen atoms are omitted for clarity.

bond length, average 2.398 Å, is reportedly one of the shortest for four-coordinated Al and P compounds. Comparable Al−P distances are found in the mixed-metal, P-bridged, four-membered ring $(Et_2O)_2Li[\mu\text{-}P(SiMe_3)_2]_2AlH_2$,[2b] 2.4001(13) Å, in the monomeric base-stabilized adduct $[H_2AlPMes_2]{\cdot}NMe_3$,[5] 2.409(3) Å, and in the aluminaphosphacubane $[i\text{-}BuAl(\mu_3\text{-}PSiPh_3)]_4$,[12a] 2.414(4) Å. In sterically crowded derivatives of $\{(Me_3Si)_3Al\}$ somewhat longer Al−P bond lengths are reported for the dimers $[(Me_3Si)_2AlPPh_2]_2$, 2.446(4) Å, and $[(Me_3Si)_2AlP(SiMe_3)Ph]_2$, 2.466(2) Å, and trimer $[(Me_3Si)_2AlP(H)(c\text{-}C_6H_{11})]_3$, 2.444(4) Å.[1c] A similar Al−P bond length range is observed for the dimers $[Et_2AlP(SiMe_3)_2]_2$,[12b] 2.460(1) Å, $[Me_2AlP(SiMe_3)_2]_2$,[12c] 2.460(1) Å, and $[Bu^i{}_2AlP(SiMe_3)_2]_2$,[12d] 2.469(2) Å, the six-membered ring compounds $[Me_2AlCH_2PMe_2]_2$,[12e] 2.451(2) Å, and $[ClAl(CH_2PMe_2)_2]_2$,[12e] 2.425(1) Å, and in the gas phase for the trimer $[Me_2AlPMe_2]_3$,[12f] 2.434(4) Å. On the other hand, in the complex cage structure of $[P_4(Cp^*Al)_6]$ the Al−P distances for the four-coordinated P atoms average 2.406 Å while for the tricoordinated P atoms they average 2.327 Å; further, in the zinc blende structure of AlP this distance has the value of 2.35 Å.[13] It is instructive to compare all these bond lengths with the recently published ab initio calculations of the structures of the dimer $[H_2AlPH_2]_2$ and cubic cluster $[HAlPH]_4$ that provided the Al−P distances of 2.451 and 2.434 Å, respectively.[14]

The structure of the monomeric base-stabilized adduct $[H_2AlAs(SiMe_3)_2]{\cdot}NMe_3$ (**2**) is one of the rare authenticated aluminum−arsenic compounds and is the first reported for the parent AlH_2-containing alane arsenide (Figure 2). The characteristic feature of this structure is that it contains four-coordinated aluminum bonded to three-coordinated arsenic. This could partially explain the fact that the Al−As bond length in **2**, 2.4383(21) Å, is very short and, actually, is the shortest bond of this type reported to date. For example, in the mixed-metal, As-bridged, four membered-ring $(Et_2O)_2Li[\mu\text{-}As(SiMe_3)_2]_2AlH_2$ this distance is at 2.4934(7) Å.[2b] Distances longer than that are found in the dimers $[Et_2AlAs(t\text{-}Bu)_2]_2$,[15a] average 2.567 Å, $[Et_2AlAs(SiMe_3)_2]_2$,[15b] average 2.535 Å, and trimers $[Me_2AlAsPh_2]_3{\cdot}(C_7H_8)_2$,[15c] average 2.524 Å, $[Me_2AlAs(CH_2SiMe_3)Ph]_3$,[15c] average 2.518 Å (2.504(5) $Å_{min}$−2.526(5) $Å_{max}$). We note that in two other reported similar structures of the monomeric base-stabilized adducts, $[H(Cl)AlN(SiMe_3)_2]{\cdot}NMe_3$[1c] and $[H_2AlPMes_2]{\cdot}NMe_3$,[5] relatively very short Al−pnictide covalent distances are also observed. In addition to the very short Al−As distance in **2**, the dative bond length between Al and N from coordinated NMe_3, 1.998(7) Å, requires special attention. This length appears to be among the shortest for alane trimethylamine adducts. This is illustrated by the relevant dative Al−N lengths in the compounds $[H_2AlPMes_2]{\cdot}NMe_3$,[5] 2.009(8) Å, and $[H(Cl)AlN(SiMe_3)_2]{\cdot}NMe_3$,[1c] 2.016(5) Å, and in simple adducts such as $(Me_3Si)_3Al{\cdot}NMe_3$,[4b] 2.040(6) Å, and $[(Me_3Si)_3Al]_2TMEDA$,[16a] 2.069(5) Å. This bond is also shorter than the Al−N distances in the monomeric $H_3Al{\cdot}NMe_3$ (gas phase),[16b] 2.063(8) Å, and monomeric $Me_3Al{\cdot}NMe_3$ (gas phase),[16c] 2.099(10) Å. Apparently, the large effective Lewis acidity of Al in the monomeric unit $[H_2AlAs(SiMe_3)_2]$ of **2** is more efficiently fulfilled through interaction with the lone electron pair on nitrogen in NMe_3 than with the available electron pair on the neighboring arsenic. The presence of the latter electron pair can be inferred from the pyramidal configuration of ligands around arsenic (sum of angles, 298.1°).

In the first approximation, compounds **1** and **2** seem to be good precursors for pyrolytic conversion to AlP and AlAs, respectively, via dehydrosilylation. In the case of **2**, the conversion would additionally require that the coordinated NMe_3 is efficiently removed without significantly influencing the target elimination chemistry. We note, however, that our observations concerning the compounds' stabilities indicate that, in addition to $HSiMe_3$ elimination, thermally enhanced ligand redistribution may take place resulting in the formation of $E(SiMe_3)_3$ and therefore altering the nature of products. Additionally, although not observed in this study at ambient conditions, reductive decomposition with the evolution of dihydrogen and formation of elemental aluminum, a common decomposition pathway for alanes,[17] may become significant at higher temperatures as well. For example, regarding the latter aspect, one of the compounds discussed above, $[H_2AlPMes_2]{\cdot}NMe_3$, was reported as an OMCVD source to deposit aluminum films.[5] Such a decomposition pathway above, however, could be due to likely higher energy barriers of mesitylene formation under specific CVD conditions than trimethylsilane formation in our bulk decomposition. To assess the feasibility of the conversion of **1** and **2** to AlP and AlAs, respectively, exploratory pyrolysis experiments were carried out.

The pyrolysis of **1** was performed at 450 and 950 °C under vacuum. The experiment at 450 °C was done with collection and analysis of volatiles. The volatiles consisted of $HSiMe_3$, CH_4, and H_2; small amounts of an oily colorless liquid, likely

(12) (a) Cowley, A. H.; Jones, R. A.; Mardones, M. A.; Atwood, J. L.; Bott, S. G. *Angew. Chem., Int. Ed. Engl.* **1990**, *29*, 1409. (b) Wells, R. L.; McPhail, A. T.; Self, M. F.; Laske, J. A. *Organometallics* **1993**, *12*, 3333. (c) Hey-Hawkins, E.; Lappert, M. F.; Atwood, J. L.; Bott, S. G. *J. Chem. Soc., Dalton Trans.* **1991**, 939. (d) Krannich, L. K.; Watkins, C. L.; Schauer, S. J.; Lake, C. H. *Organometallics* **1996**, *15*, 3980. (e) Karsch, H. H.; Appelt, A.; Köhler, F. H.; Müller, G. *Organometallics* **1985**, *4*, 231. (f) Haaland, A.; Hougen, J.; Volden, H. V.; Hanika, G. H.; Karsch, H. H. *J. Organomet. Chem.* **1987**, *322*, C24.

(13) Dohmeier, C.; Schnöckel, H.; Robl, C.; Schneider, U.; Ahlrichs, R. *Angew. Chem., Int. Ed. Engl.* **1994**, *33*, 199.

(14) Davy, R. D.; Schaefer, H. F., III. *J. Phys. Chem. A* **1997**, *101*, 5707.

(15) (a) Heaton, D. E.; Jones, R. A.; Kidd, K. B.; Cowley, A. H.; Nunn, C. M. *Polyhedron* **1988**, *7*, 1901. (b) Wells, R. L.; McPhail, A. T.; Speer, T. M.; *Organometallics* **1992**, *11*, 960. (c) Laske-Cooke, J. A.; Purdy, A. P.; Wells, R. L.; White, P. S. *Organometallics* **1996**, *15*, 84.

(16) (a) Goebel, D. W.; Hencker, J. L.; Oliver, J. P. *Organometallics* **1983**, *2*, 746. (b) Almenningen, A.; Gundersen, G.; Haugen, T.; Haaland, A. *Acta Chem. Scand.* **1972**, *26*, 3928. (c) Anderson, G. A.; Almenningen, A.; Forgaard, F. R.; Haaland, A. *J. Chem. Soc., Chem. Commun.* **1971**, 480.

(17) For example, see review: Jones, C.; Koutsantonis, G. A.; Raston, C. L. *Polyhedron* **1993**, *12*, 1829.

$P(SiMe_3)_3$, were also observed to distill out. The presence of $HSiMe_3$ was expected from the target dehydrosilylation chemistry, but the remaining compounds pointed out also to other decomposition pathways. In regard to that, methane and hydrogen were commonly observed during pyrolysis of $SiMe_3$-containing precursors although significant quantities of the latter were observed at still higher temperatures,[1b,2c,18] and hydrogen could additionally be formed via reductive decomposition of the AlH_2 groups. The brown solid product from this experiment showed by XRD spectroscopy the onset of AlP crystallinity. On the other hand, the pyrolysis at 950 °C afforded a black solid that was shown to contain the nanocrystalline cubic AlP with 5 nm average crystallite size. The elemental analysis yielded Al/P ratio 1, consistent with the AlP stoichiometry, but also significant proportions of residual Si and C. On the basis of these observations, we concluded that the formation of AlP from dehydrosilylation was accompanied by side-decomposition of residual $SiMe_3$ and AlH_2 (likely) groups. Also, compound **1** (or derived byproducts) must have volatilized significantly during both pyrolyses because we observed a side-effect formation of uniform, very robust, goldenlike thin films on the entire surface of the pyrolysis tube.

The pyrolysis of **2** was performed at 450 °C under vacuum with the collection and analysis of volatiles, similarly as above. $HSiMe_3$, NMe_3, CH_4, and H_2 were detected in the volatiles, and significant quantities of condensed liquid, likely $As(SiMe_3)_3$, were observed on the cold parts of the setup as well. The condensable volatiles contained, in addition to $HSiMe_3$, some NMe_3 which we were able to identify by IR spectroscopy but unable to separate from $HSiMe_3$ and quantify due to the closeness of their vapor pressures. The black solid product was shown by XRD to contain nanocrystalline cubic AlAs with an average crystallite size of approximately 2 nm. The lack of nitrogen in the elemental analysis of the solid was consistent with an efficient removal of the amine while relatively low Si and C contents indicated a rather small-sized side-decomposition of residual $SiMe_3$ groups. The Al/As ratio of 1.78 indicated, however, significant excess of aluminum (possibly in the form of elemental Al) vs the expected ratio 1 for AlAs. This piece of data could be linked to the formation of removable $As(SiMe_3)_3$ and, therefore, depletion in arsenic of the solid product and was likely associated with the specific decomposition pathway for alanes and gallanes, namely, reductive coupling with H_2 evolution and metal formation. We point out that similar composition characteristics were previously observed in the pyrolysis of the related gallane derivative, i.e., the polymeric solid derived from unstable $[H_2GaAs(SiMe_3)_2]_3$, which yielded a product containing nanocrystalline GaAs and showing a Ga/As ratio 1.5.[2c] In summary, our preliminary pyrolysis experiments for **1** and **2** demonstrated that these precursors were subject to dehydrosilylation and could be pyrolyzed toward nanocrystalline AlP and AlAs, respectively. However, under the applied pyrolysis conditions, other decomposition pathways competed in these systems and contributed to retention of residuals containing Si and C, most likely in the form of separate (to the crystalline product) amorphous phases. In the case of **2**, the intrinsic decomposition pathway for alanes, reductive coupling, appeared to be especially pronounced and afforded the aluminum-enriched product.

Acknowledgment. R.L.W. wishes to thank the Office of Naval Research for its financial support.

Supporting Information Available: Text providing information on collection of data and refinement, crystal packing diagrams, and tables of bond distances, bond and torsion angles, anisotropic temperature factor parameters, and atomic fractional coordinates for **1** and **2** (12 pages). Ordering information is given on any current masthead page.

IC980218A

(18) Janik, J. F.; Baldwin, R. A.; Wells, R. L.; Pennington, W. T.; Schimek, G. L.; Rheingold, A. L.; Liable-Sands, L. M. *Organometallics* **1996**, *15*, 5385.